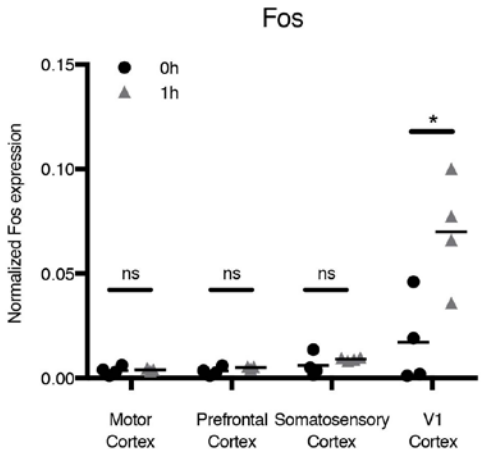

Supplementary Figure 1

***Fos* induction by visual stimulus is restricted to V1**

Fos expression measured by RT-qPCR at 0 and 1 h conditions following inDrops sample preparation in 4 brain tissues. *p=0.021, unpaired t-test, two-sided. n=4 animals for all 0 h samples, n=3 animals for 1 h motor and prefrontal cortex, n=4 animals for 1 h somatosensory and visual cortex. Bar indicates mean.

a

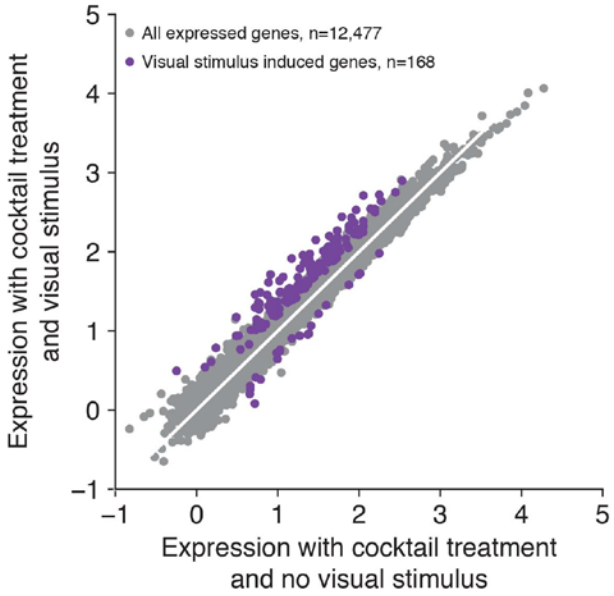

b

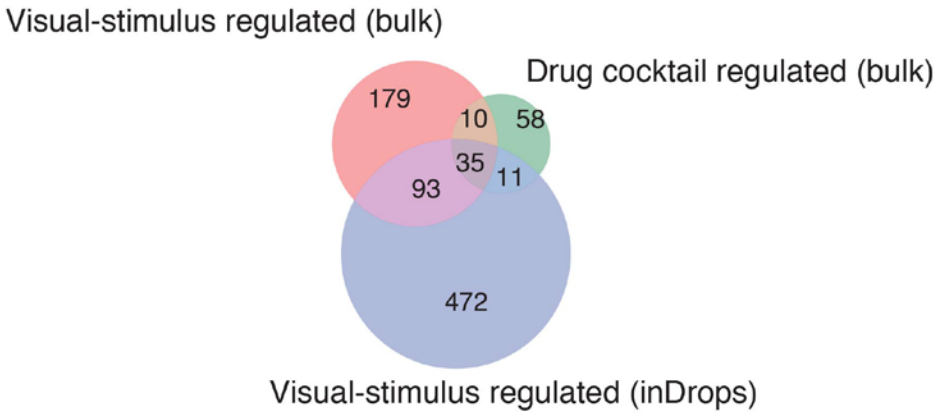

Supplementary Figure 2

Drug cocktail does not grossly alter transcription in visual cortex as measured by bulk RNA-seq

(**a**) Scatter plot of gene expression (log10 [TMM-normalized CPM + .01]) for 12,477 genes in visual cortex from drug-cocktail-perfused animals that were dark- (0 h) or light- (1 h) exposed (n=4 animals for each condition). 168 significantly differentially expressed genes (DEG) corresponding to the bulk visual experience-dependent program are denoted in purple (FDR<.01, fold change >=2, limma, Online Methods).
(**b**) Venn diagram demonstrating the overlap of the following three gene sets (in clockwise order): DEG from panel A, DEG from **Fig. 1d**, and the 611 cell-type-specific DEG from **Fig. 2b**. Approximately one half of genes (56/114) that are repressed by the cocktail were identified as visual-stimulus induced in either the bulk or single-cell RNA-seq experiments. GO analysis results for all 114 genes are listed in **Supplementary Table 1**.

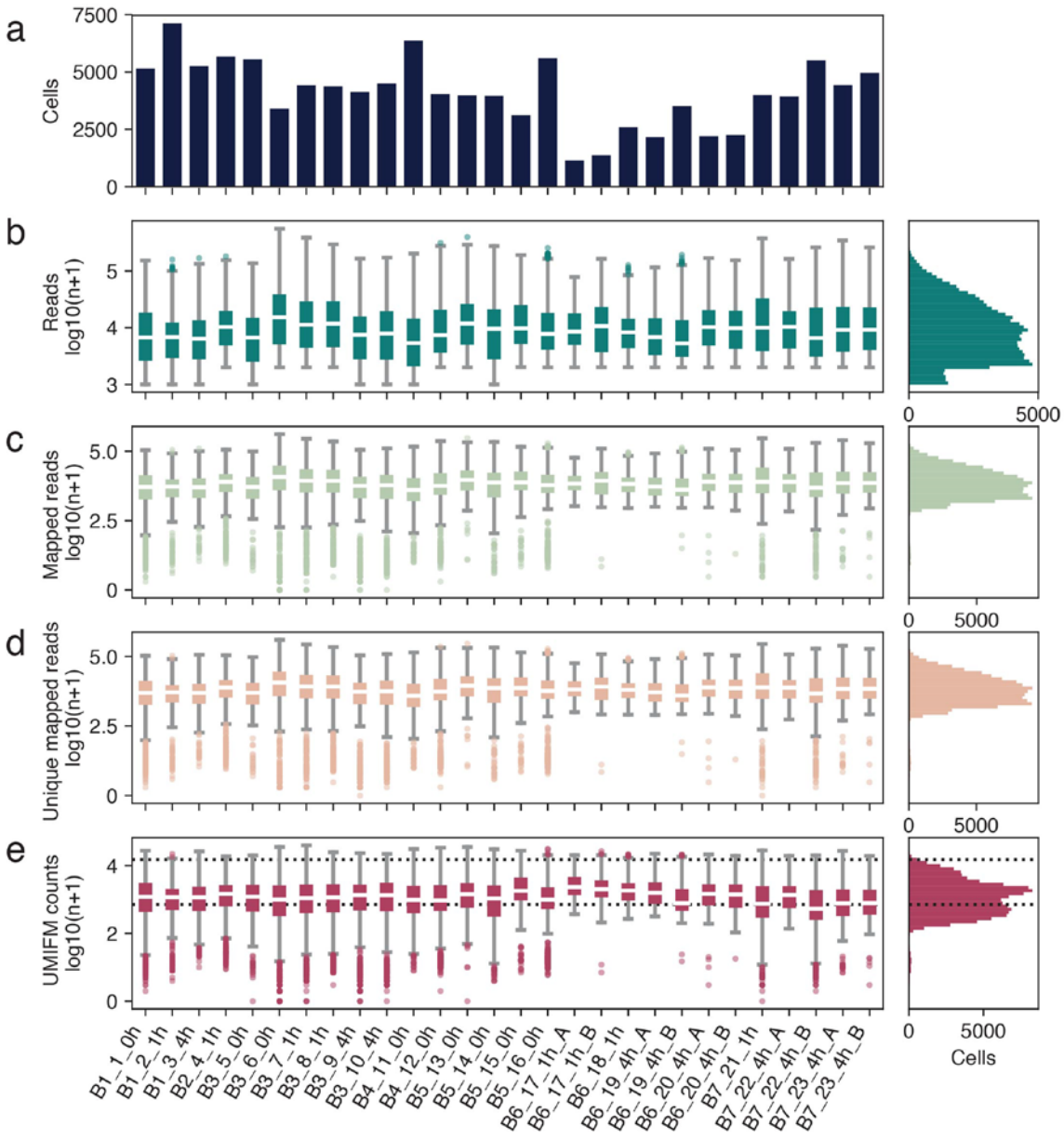

Supplementary Figure 3

inDrops sample sequencing metrics

The samples described in the manuscript comprise 28 libraries collected across 23 animals denoted by the sample names along the x-axis. All panels in this figure represent sequencing metrics across all cells with ≥1,000 total reads (cells=114,601). For each metric, whisker plots demarcate quartiles. Data outside 1.5-times the interquartile range (Q3-Q1) were labeled as dots. The median of each distribution is marked in white (left). Each distribution is also aggregated across all samples and this histogram is plotted.
(**a**) Number of cells collected by sample.
(**b**) Total reads per cell by sample.
(**c**) Total mapped reads per cell by sample.
(**d**) Reads mapping to a unique genomic location per cell by sample
(**e**) UMI filtered, uniquely mapping counts per cell by sample.

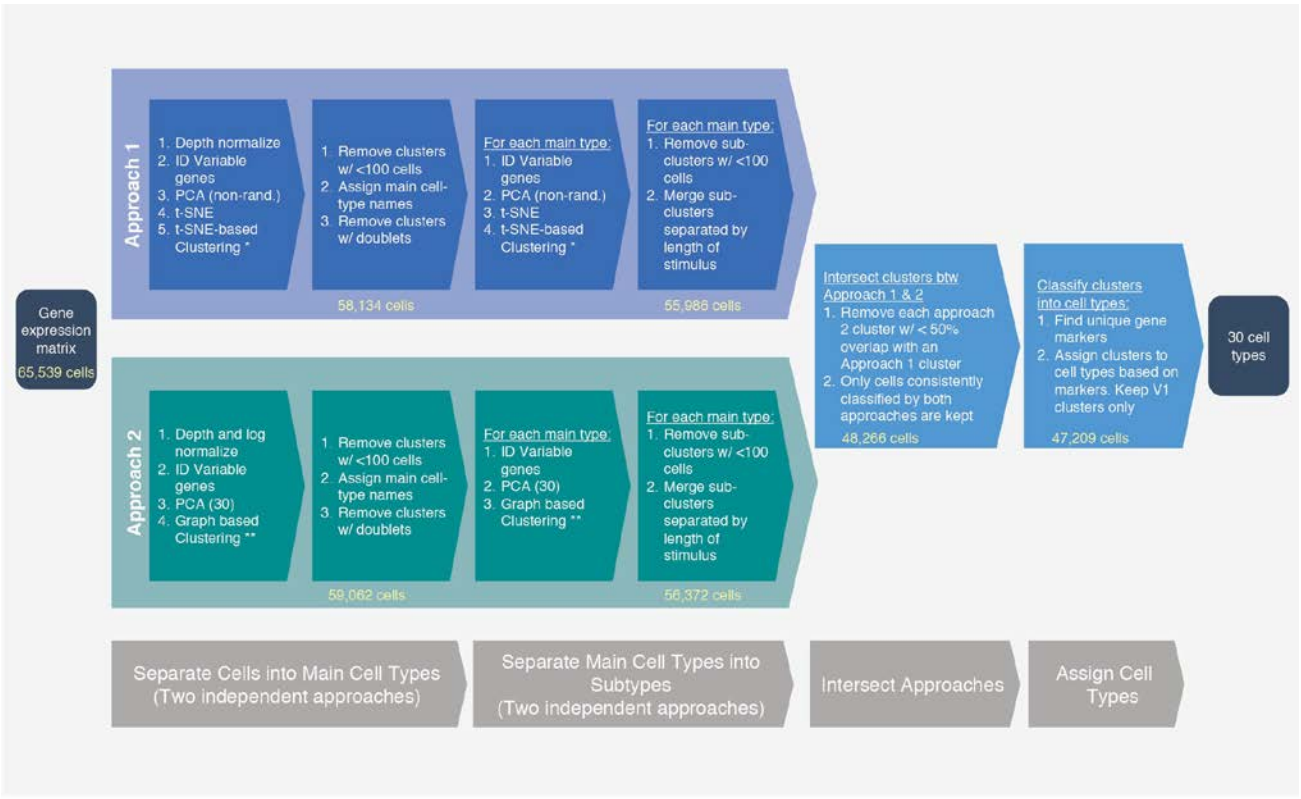

Supplementary Figure 4

Flowchart of bioinformatics clustering and cell-type assignment
Workflow diagram showing bioinformatic clustering and cell-type assignment pipeline (Online Methods). The number of cells passing each stage of the pipeline are indicated in light yellow.

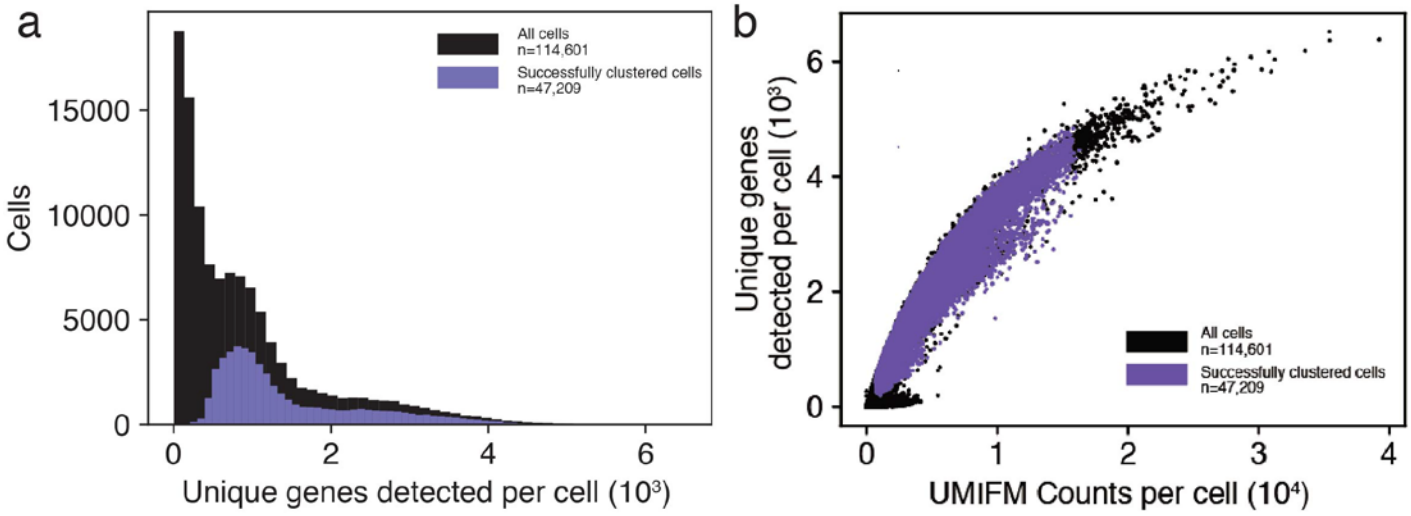

Supplementary Figure 5

inDrops sample gene detection metrics

(**a**) The number of unique genes detected per cell for all cells acquired with ≥1,000 reads per cell (cells=114,601, black), and for the subset of cells that were successfully assigned a cell type designation (cells=47,209, purple) as a histogram.
(**b**) Same data plotted on a scatter plot showing unique genes per cell as a function of UMIFM counts per cell.

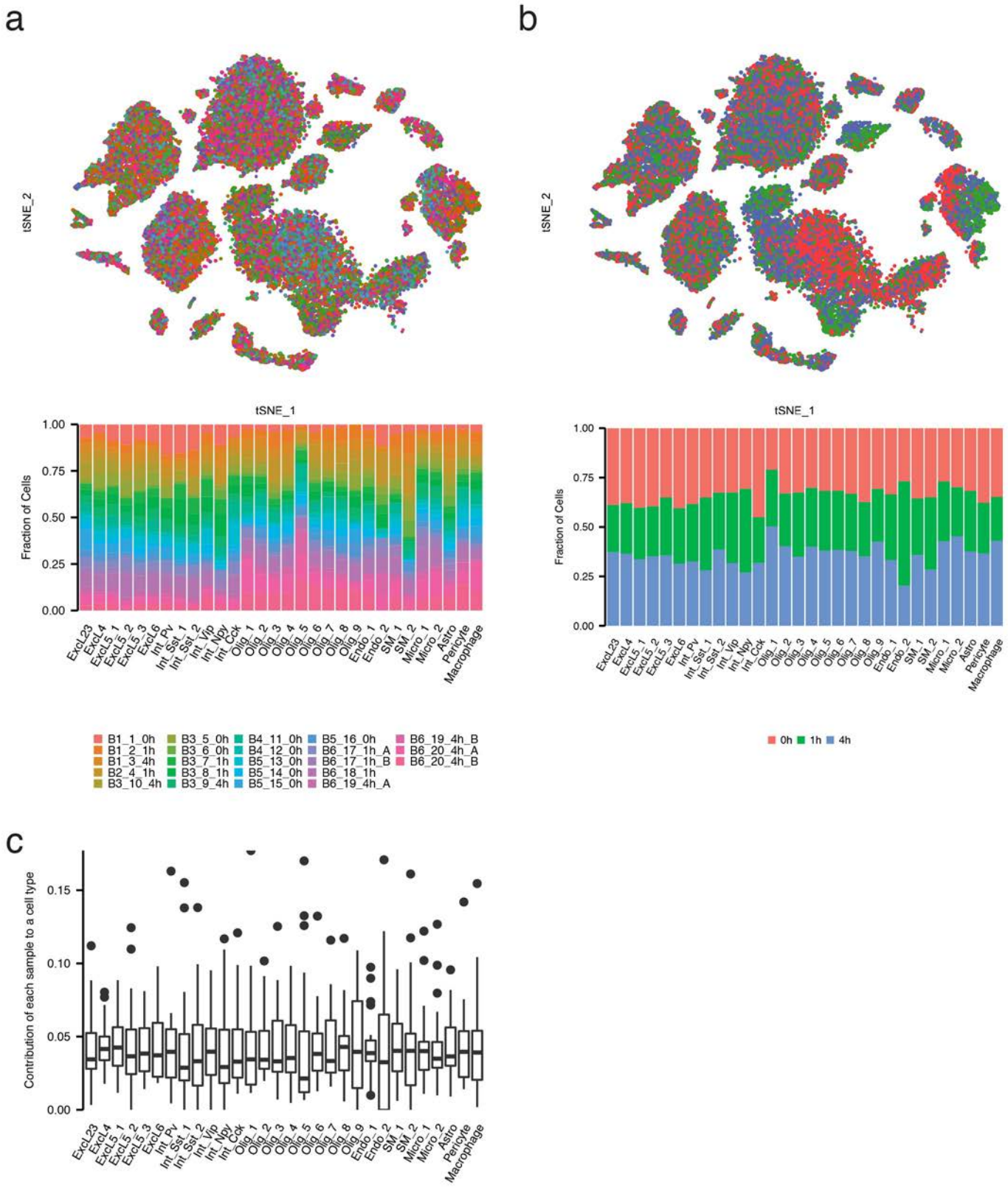

Supplementary Figure 6

Samples and stimulus conditions are evenly distributed across cell types

(**a**) Distribution of 23 samples across 30 cell types shown on top of total t-SNE (top) and denoted as fraction of cells for each cell type (bottom).
(**b**) Same plots showing distribution of stimulus paradigm across 23 samples and 30 cell types.
(**c**) Quantification of the distribution shown in (**a**) Box plot with median (Tukey). Data outside 1.5-times the interquartile range (Q3-Q1) were labeled as dots.

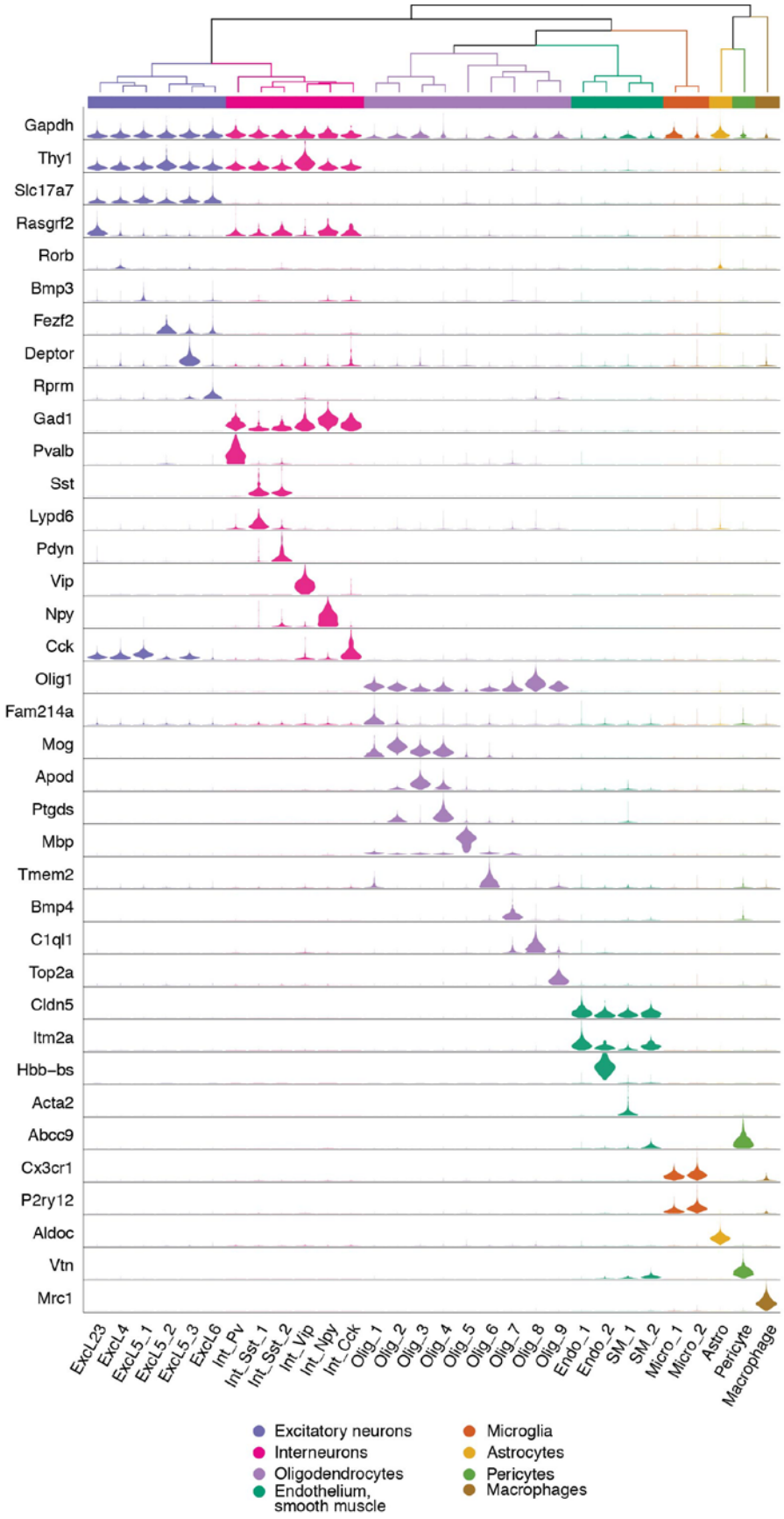
Gapdh
Thy1
Slc17a7
Rasgrf2
Rorb
Bmp3
Fezf2
Deptor
Rprm
Gad1
Pvalb
Sst
Lypd6
Pdyn
Vip
Npy
Cck
Olig1
Fam214a
Mog
Apod
Ptgds
Mbp
Tmem2
Bmp4
C1ql1
Top2a
Cldn5
Itm2a
Hbb−bs
Acta2
Abcc9
Cx3cr1
P2ry12
Aldoc
Vtn
Mrc1
ExcL23
ExcL4
ExcL5_1
ExcL5_2
ExcL5_3
ExcL6
Int_Pv
Int_Sst_1
Int_Sst_2
Int_Vip
Int_Npy
Int_Cck
Olig_1
Olig_2
Olig_3
Olig_4
Olig_5
Olig_6
Olig_7
Olig_8
Olig_9
Endo_1
Endo_2
SM_1
SM_2
Micro_1
Micro_2
Astro
Pericyte
Macrophage
Excitatory neurons
Interneurons
Oligodendrocytes
Endothelium, smooth muscle
Microglia
Astrocytes
Pericytes
Macrophages

Supplementary Figure 7

Expression of marker genes across all cell types
Dendrogram of cell types and violin plots showing the distribution of expression of selected marker genes across all 30 analyzed cell types. Cell types are hierarchically clustered based on gene expression across all variable genes.

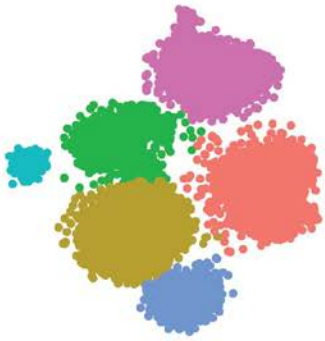

Excitatory Neurons
- ExcL23
- ExcL4
- ExcL5_1
- ExcL5_2
- ExcL5_3
- ExcL6

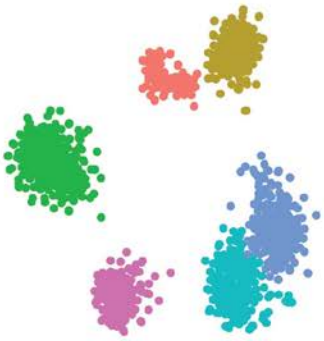

Interneurons
- Int_Cck
- Int_Npy
- Int_Pv
- Int_Sst_1
- Int_Sst_2
- Int_Vip

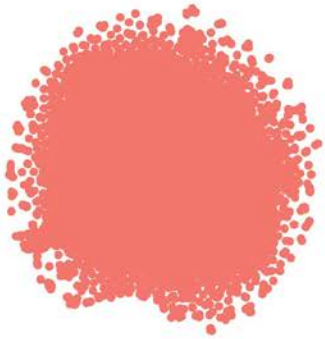

Astrocytes
- Astro

Oligodendrocytes
- Olig_1
- Olig_2
- Olig_3
- Olig_4
- Olig_5
- Olig_6
- Olig_7
- OPC_1
- OPC_2

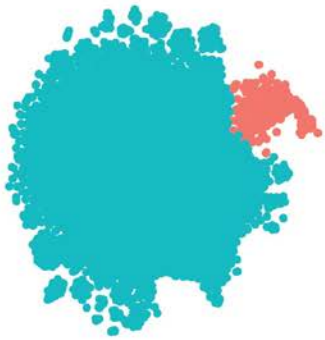

Microglia
- Micro_1
- Micro_2

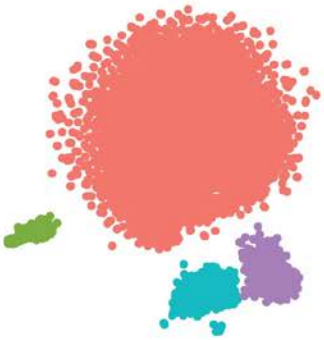

Endothelium, smooth muscle
- Endo_1
- Endo_2
- SM_1
- SM_2

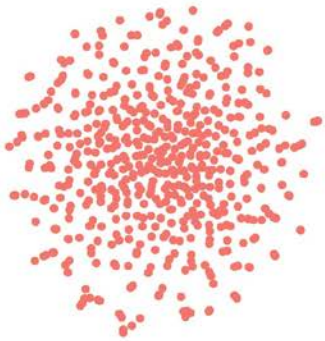

Macrophages
- Macrophage

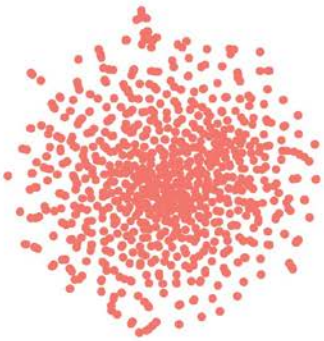

Pericytes
- Pericyte

Supplementary Figure 8

t-SNE plots separating cell-types within each main cell class

t-SNE plots are shown for each of the eight main cell types: excitatory neurons (14287 cells), inhibitory neurons (936 cells), astrocytes (7039 cells), oligodendrocytes and oligodendrocyte precursor cells (OPCs; 10,456 cells), microglia (10158 cells), endothelial and smooth muscle cells (4071 cells), macrophages (537 cells), and pericytes (782 cells). Colors within each plot indicate different subtypes.

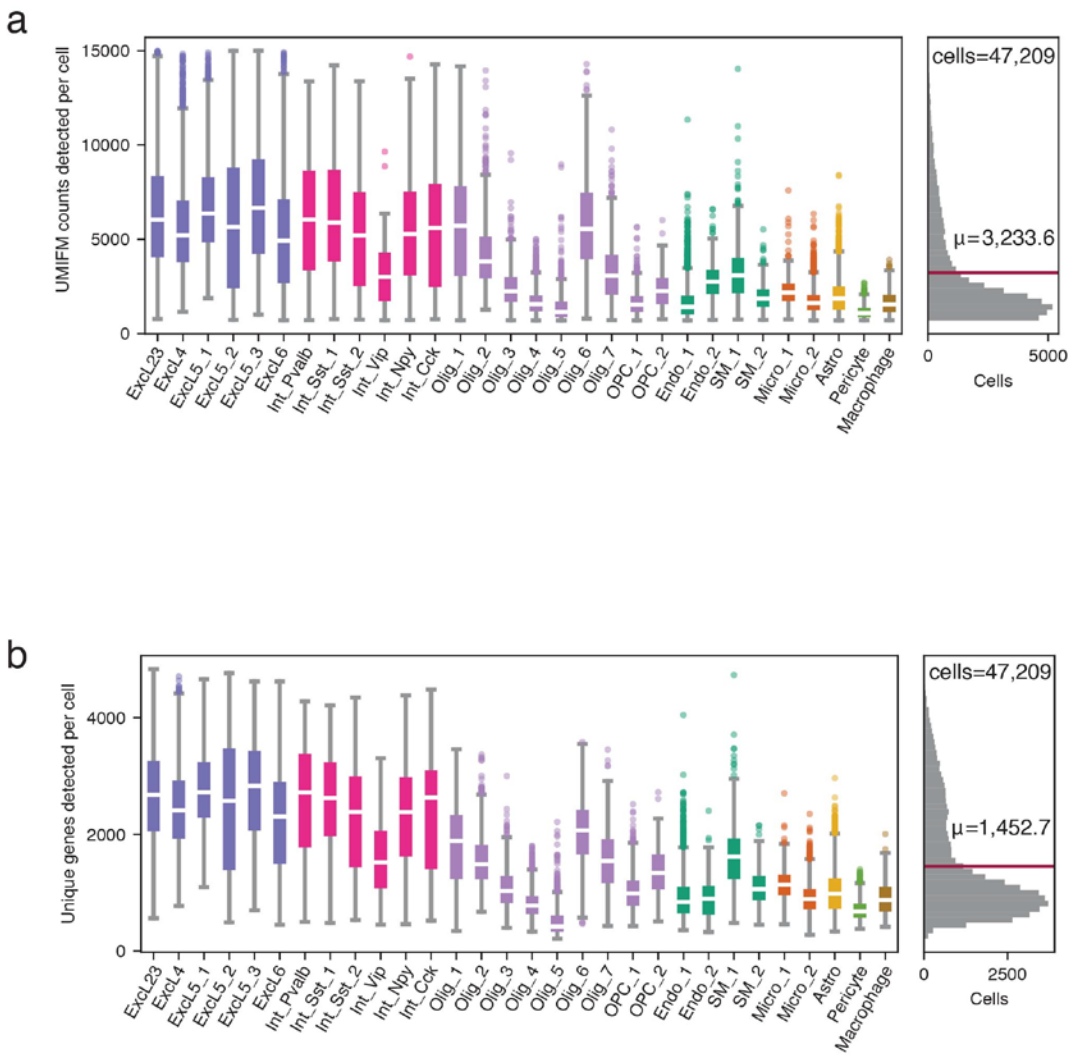

Supplementary Figure 9

UMIFM counts and genes detected per cell by cell type

Distributions of (**a**) UMIFM counts per cell and (**b**) unique genes detected per cell plotted by cell type as whisker plots showing quartiles (median in white) for all cells that were successfully assigned to a cell type (cells=47209, left). Summary histograms (right) show the relevant metric aggregated across all clustered cells with means denoted by the red line. Across the 47209 clustered cells, an average of 3233.6 UMIFM counts and 1452.7 genes were obtained per cell. Data outside 1.5-times the interquartile range (Q3-Q1) were labeled as dots.

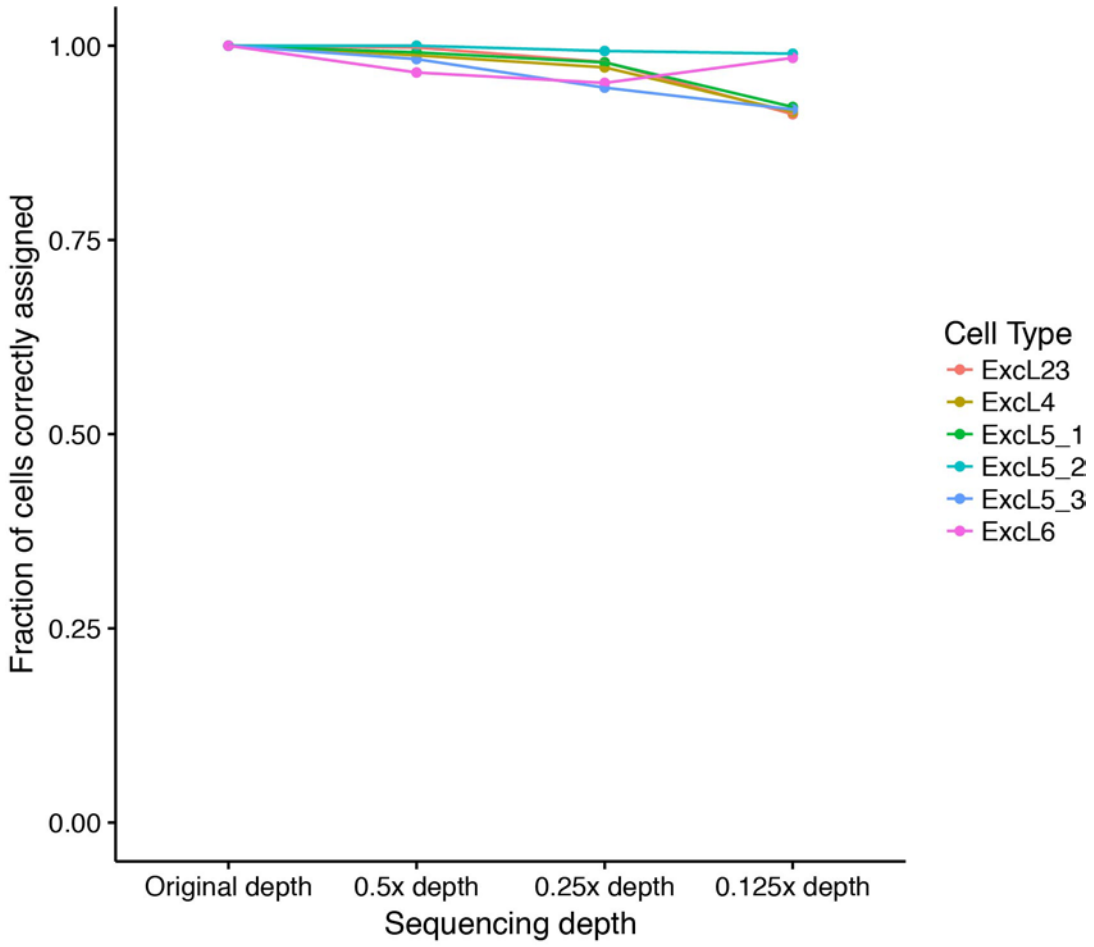

Supplementary Figure 10

Dependence of clustering on sequencing depth

All excitatory neurons (L23, L4, L5_1, L5_2, L5_3 and L6, total cell number=13,230, average UMI per cell=6,020) were pooled and three additional datasets created by randomly subsampling each cell to contain ½, ¼ or ⅛ its starting number of transcripts. All four datasets were analyzed and clustered independently using Seurat. Marker genes were used to assign each new cluster back to one of the original excitatory cell types (L23, L4, L5_1, L5_2, L5_3 and L6). Graph shows the fraction of cells in each cluster derived from the subsetted data that were correctly assigned to the original cluster in the non-subsetted dataset.

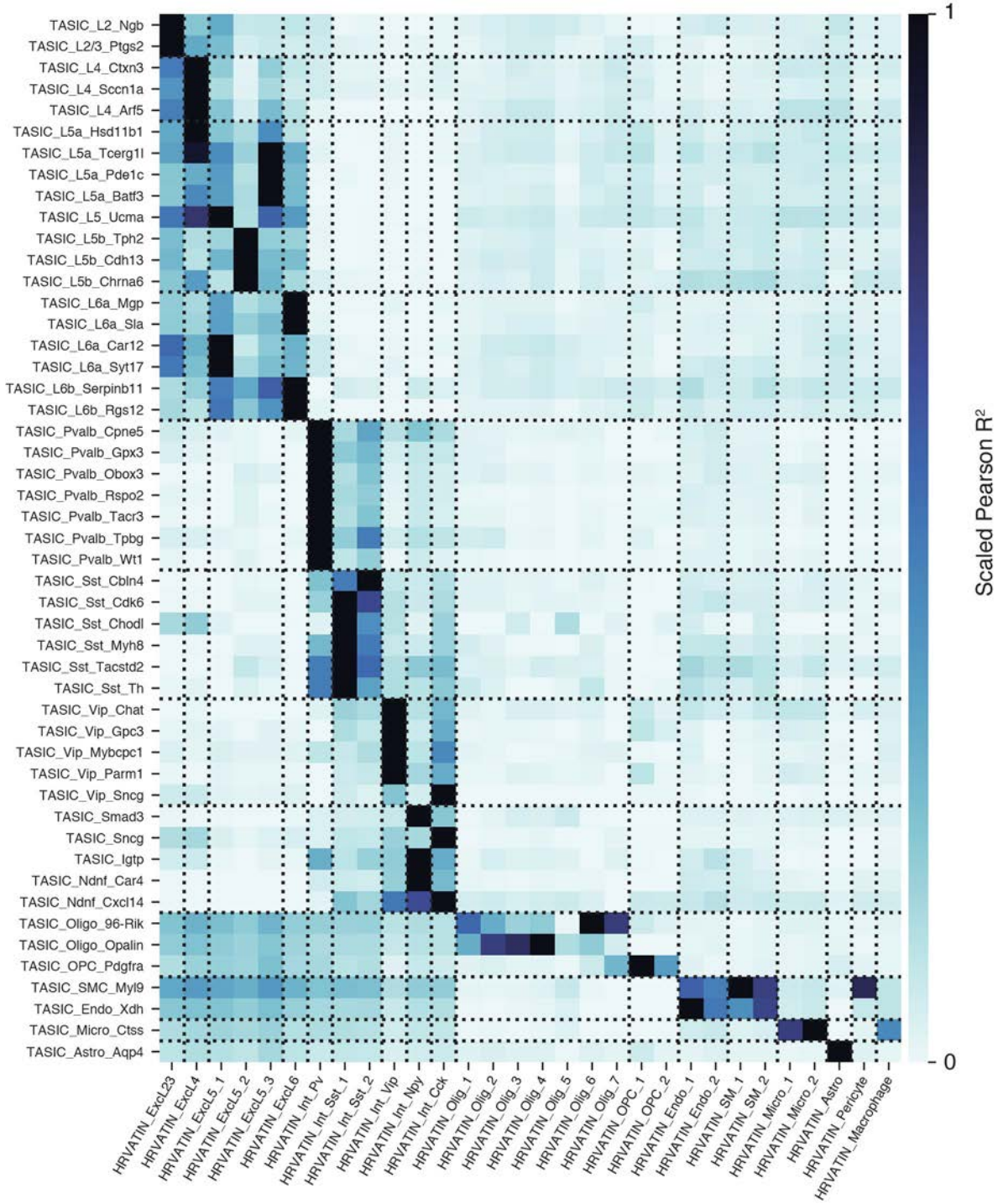

Supplementary Figure 11

Correlations between inDrops- and Tasic et al.-identified cell types

Heatmap of pairwise Pearson R^2 correlations between all cell types identified in Ref. [23] and this study. Magnitude of correlation denoted by color intensity as shown on scale bar. For clarified representation, values are scaled such that the highest obtained R^2 across each TASIC-labeled cell type is 1. Broadly defined cell types within each of the two studies are demarcated by dotted lines.

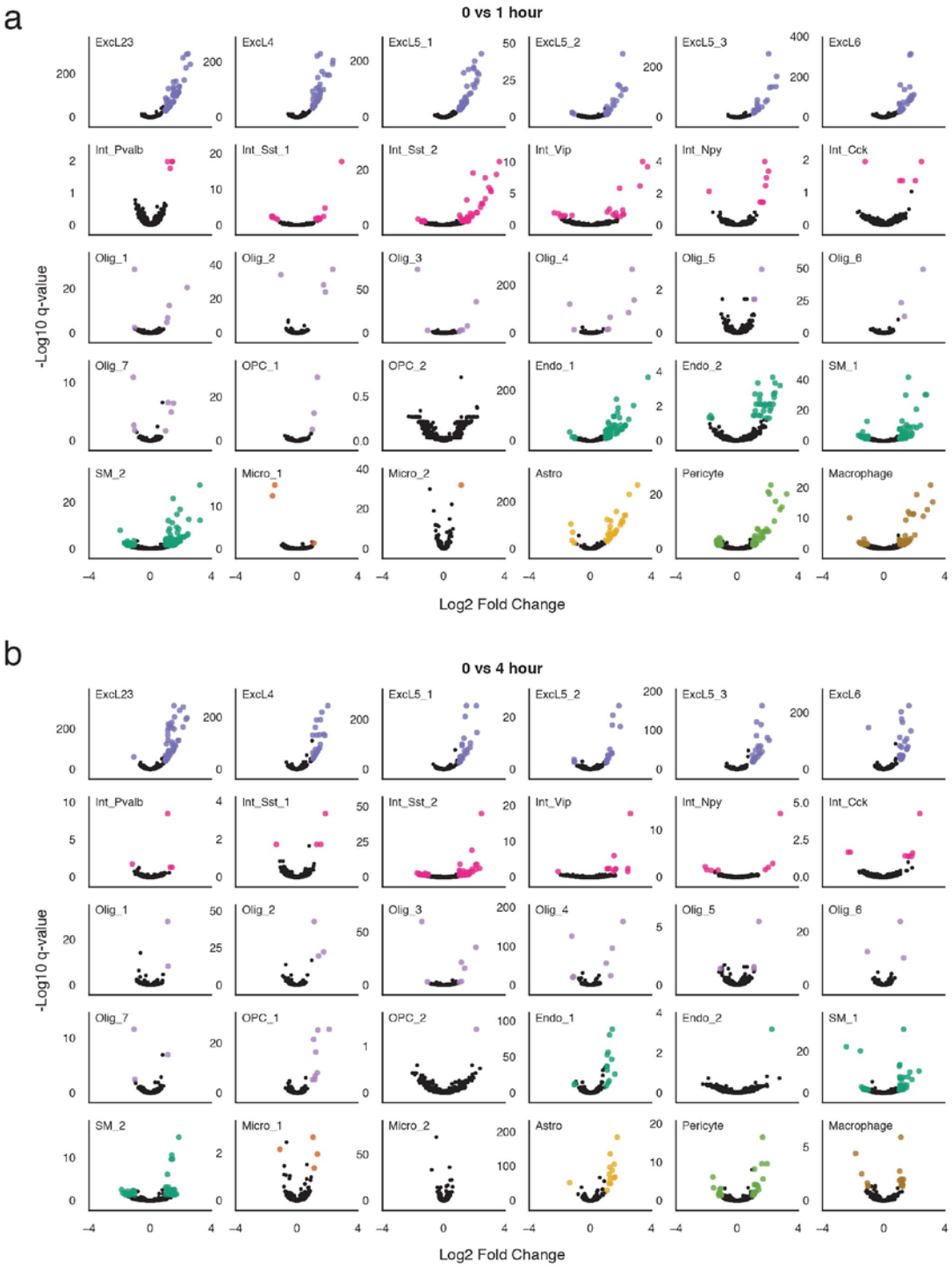

Supplementary Figure 12

Differential expression analysis results by stimulus for all cell types

Volcano plots of –log10 Monocle2 derived q-values against log2 fold change between 0 and 1 h (**a**) and 0 and 4 h (**b**) stimulus comparisons. Cells that passed FDR<.05 and |log2FC|>1 thresholds are shown in their representative colors. Number of cells for the 0, 1, 4h condition respectively: ExcL23 = 1150, 706, 1107; ExcL4 = 1211, 819, 1168; ExcL5_1 = 795, 516, 665; ExcL5_2 = 162, 104, 144; ExcL5_3 = 493, 412, 502; ExcL6 = 1328, 916, 1032; Int_Pv = 87, 66, 74; Int_Sst_1 = 61, 64, 49; Int_Sst_2 = 59, 52, 70; Int_Vip = 41,

45, 40; Int_Npy = 42, 58, 37; Int_Cck = 41, 21, 29; Olig_1 = 128, 175, 307; Olig_2 = 318, 257, 389; Olig_3 = 275, 275, 296; Olig_4 = 1220, 1204, 1623; Olig_5 = 237, 225, 285; Olig_6 = 248, 236, 302; Olig_7 = 209, 182, 239; OPC_1 = 645, 472, 608; OPC_2 = 31, 27, 43; Endo_1 = 1111, 1107, 1109; Endo_2 = 33, 65, 25; SM_1 = 115, 92, 116; SM_2 = 104, 109, 85; Micro_1 = 148, 166, 235; Micro_2 = 2873, 2381, 4355; Astro = 2234, 2156, 2649; Pericyte = 295, 200, 287; Macrophage = 187, 119, 231.

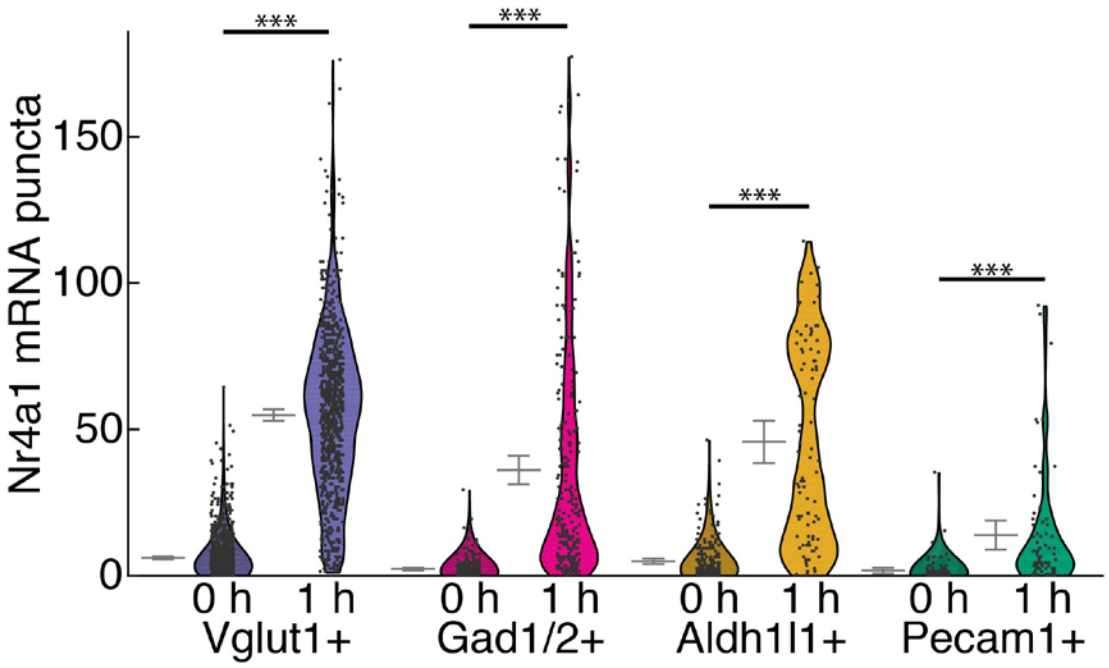

Supplementary Figure 13

***Nr4a1* is induced across multiple cell types as measured by FISH**

Nr4a1 expression as measured by FISH in 0 and 1 h stimulus conditions in excitatory (*Vglut1*+, $cells_{0h}$=987, $cells_{1h}$=778) and inhibitory (*Gad1/2*+, $cells_{0h}$=238, $cells_{1h}$=243) neurons, astrocytes (*Aldh1l1*+, $cells_{0h}$=220, $cells_{1h}$=89), and endothelial and smooth muscle cells (*Pecam1*+, $cells_{0h}$=82, $cells_{1h}$=67). ***$p<10^{-12}$, Mann-Whitney U-test, two-sided. Mean and 95% confidence intervals denoted by gray lines.

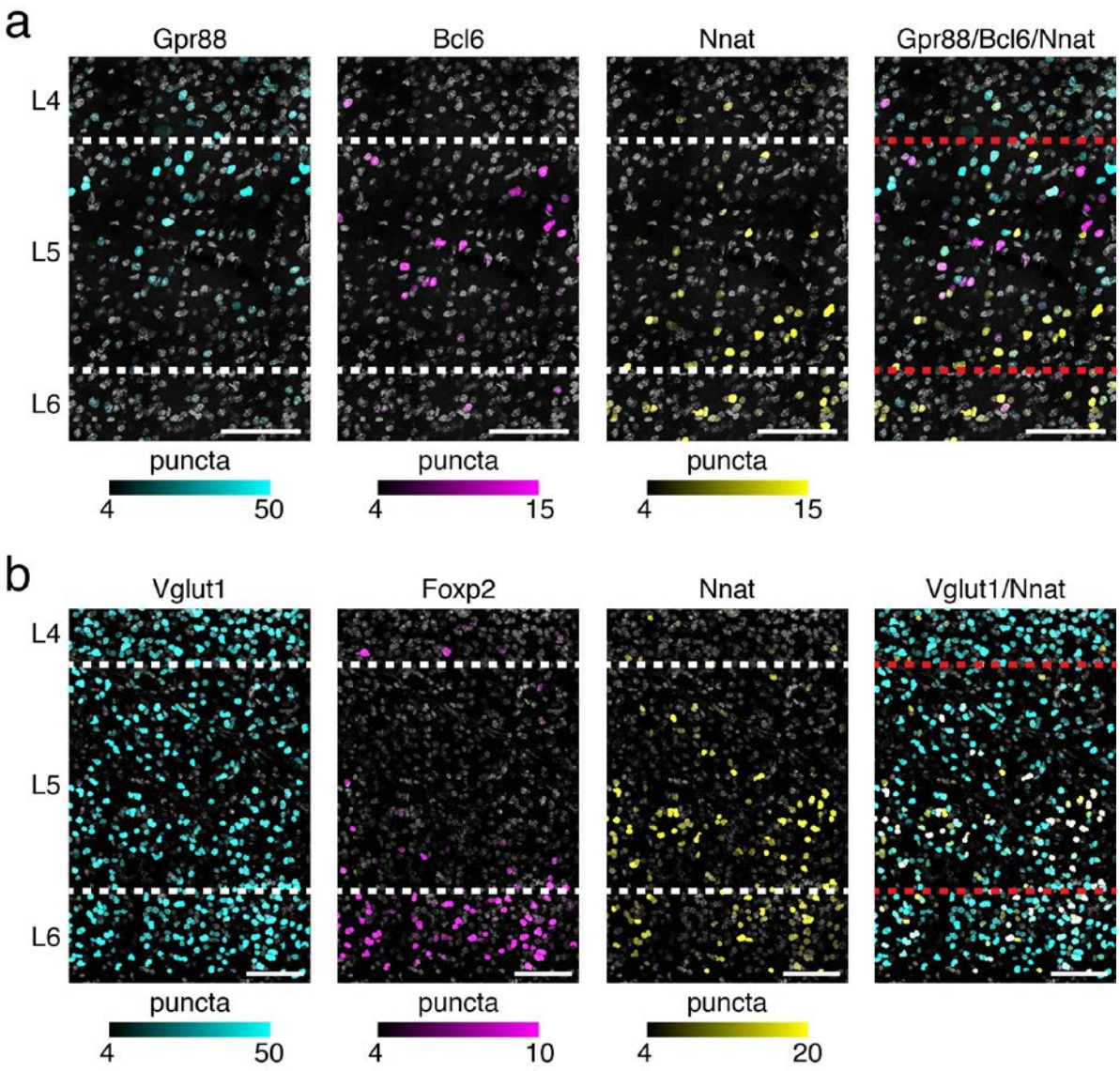

Supplementary Figure 14

Anatomical location of putative layer 5 cell types

(**a**) 3-color FISH for cell type enriched markers of ExcL5 subtypes (from left to right): Gpr88 (ExcL5_3), Bcl6 (ExcL5_2), and Nnat (ExcL5_1). The combined image (right) shows largely non-overlapping markers defining the ExcL5 subtypes. The Nnat marker labeled cells in the ventral section of layer 5 and layer 6.
(**b**) To confirm expression of Nnat across both layer 5 and 6, we carried out 3-color FISH (from left to right): Vglut1, Foxp2 (a canonical layer 6 marker), and Nnat. The presence of Vglut1/Nnat positive cells dorsal of and within Foxp2 defined layer 6 supports the layer 5/6 anatomical location of the ExcL5_1 population. Scale bars=100 um.

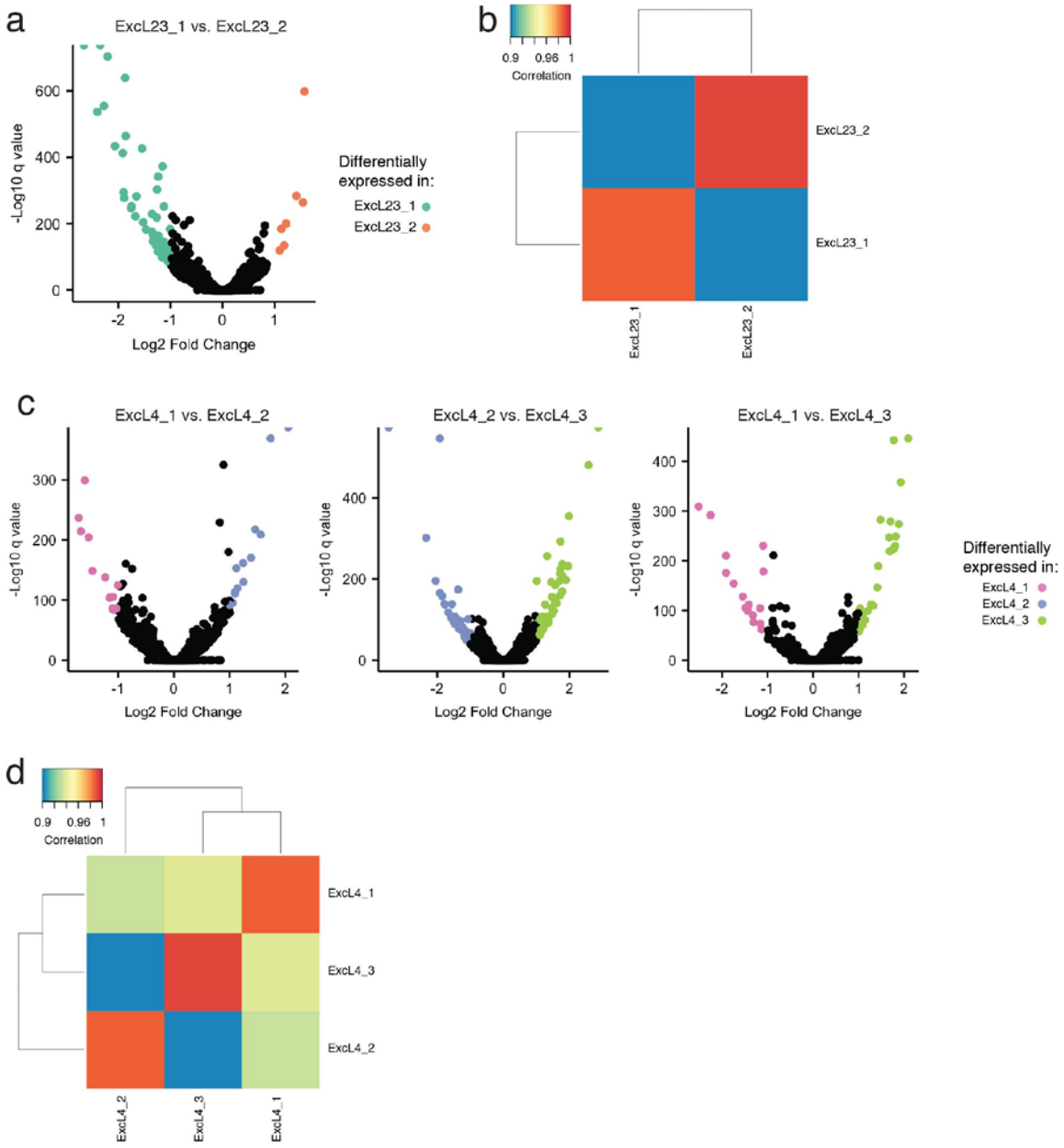

Supplementary Figure 15

Newly identified ExcL23 and ExcL4 subpopulations show differential gene expression

(**a**) 3-color FISH for cell type enriched markers of ExcL5 subtypes (from left to right): Gpr88 (ExcL5_3), Bcl6 (ExcL5_2), and Nnat (ExcL5_1). The combined image (right) shows largely non-overlapping markers defining the ExcL5 subtypes. The Nnat marker labeled cells in the ventral section of layer 5 and layer 6. Representative images from experiments on 2 cortical slices.
(**b**) To confirm expression of Nnat across both layer 5 and 6, we carried out 3-color FISH (from left to right): Vglut1, Foxp2 (a canonical layer 6 marker), and Nnat. The presence of Vglut1/Nnat positive cells dorsal of and within Foxp2 defined layer 6 supports the layer 5/6 anatomical location of the ExcL5_1 population. Scale bars=100 um. Representative images from experiments on 2 cortical slices.

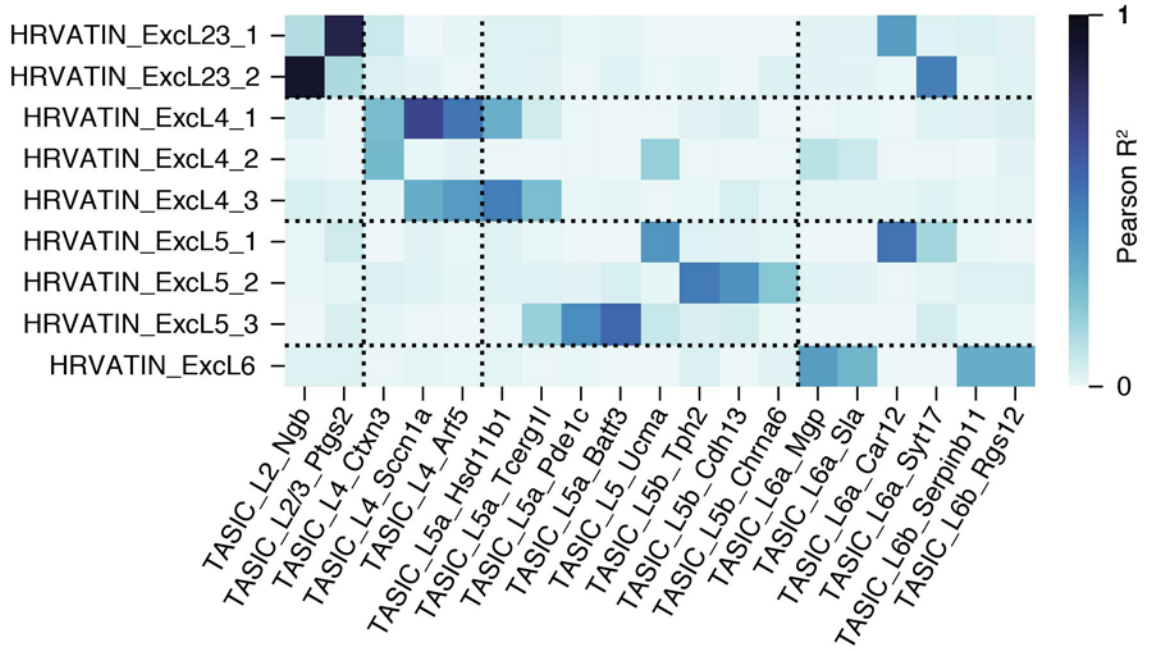

Supplementary Figure 16

Excitatory subpopulation comparison between inDrops dataset and Tasic et al.

(**a, c**) Volcano plots of –log10 Monocle2 derived FDR against log2 fold change for all genes between the two ExcL23 subpopulations (ExcL23_1/2) described in **Fig. 4c** and for all three pairwise comparisons of ExcL4 subtypes (ExcL4_1,2,3) described in **Fig. 4d** respectively. Genes that passed FDR<.05 and |log2 FC|>1 thresholds are shown in their representative colors. n_{ExcL23_1}=774, 539, 907 cells; n_{ExcL23_2}=362, 166, 193 cells; n_{ExcL4_3}=136, 137, 175 cells; n_{ExcL4_1}=732, 468, 783 cells; n_{ExcL4_2}=343, 214, 210 cells for 0, 1, and 4 h timepoints respectively.

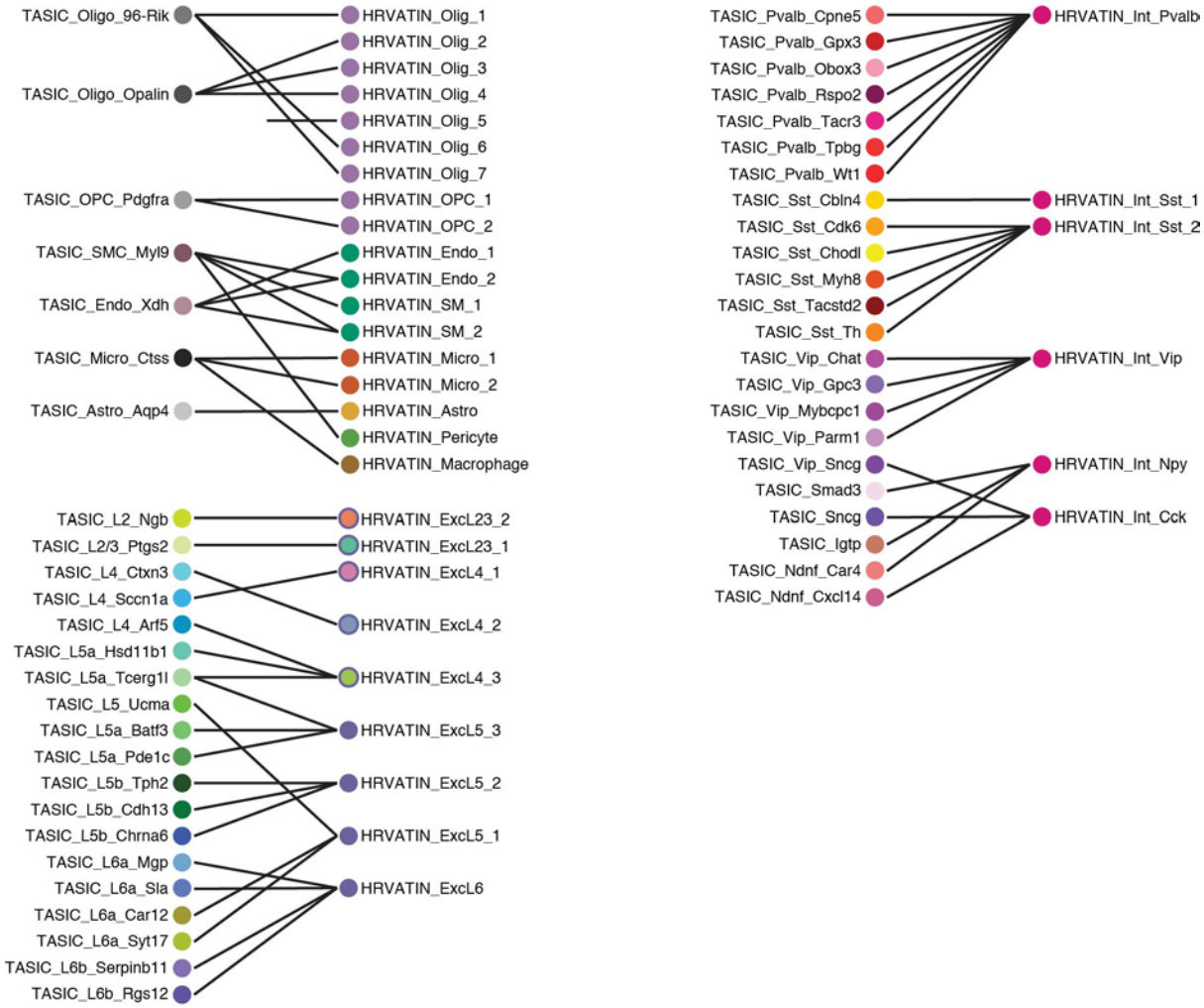

Supplementary Figure 17

Summary of inDrops- and Tasic et al.-derived cell types

A summary mapping of the Tasic et al. transcriptionally-defined cell types[23] and those described in this study constructed from analyses shown in **Supplemental Fig. 7, 11, 16, 19, 21, 22, 23**.

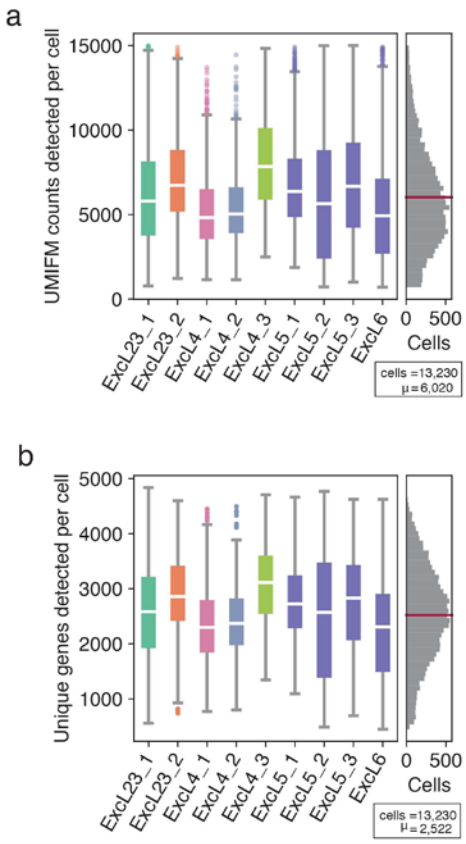

Supplementary Figure 18

Excitatory subpopulations are not defined by sequencing depth

Left: Distributions of UMIFM counts (**a**) and unique genes (**b**) detected per cell represented as whisker plots demarcating quartiles and the median (white) for each excitatory subtype across all successfully clustered excitatory cells (cells=13,230). Right: Aggregated distributions represented as histograms. Means of each metric are denoted by the red lines. Data outside 1.5-times the interquartile range (Q3-Q1) were labeled as dots.

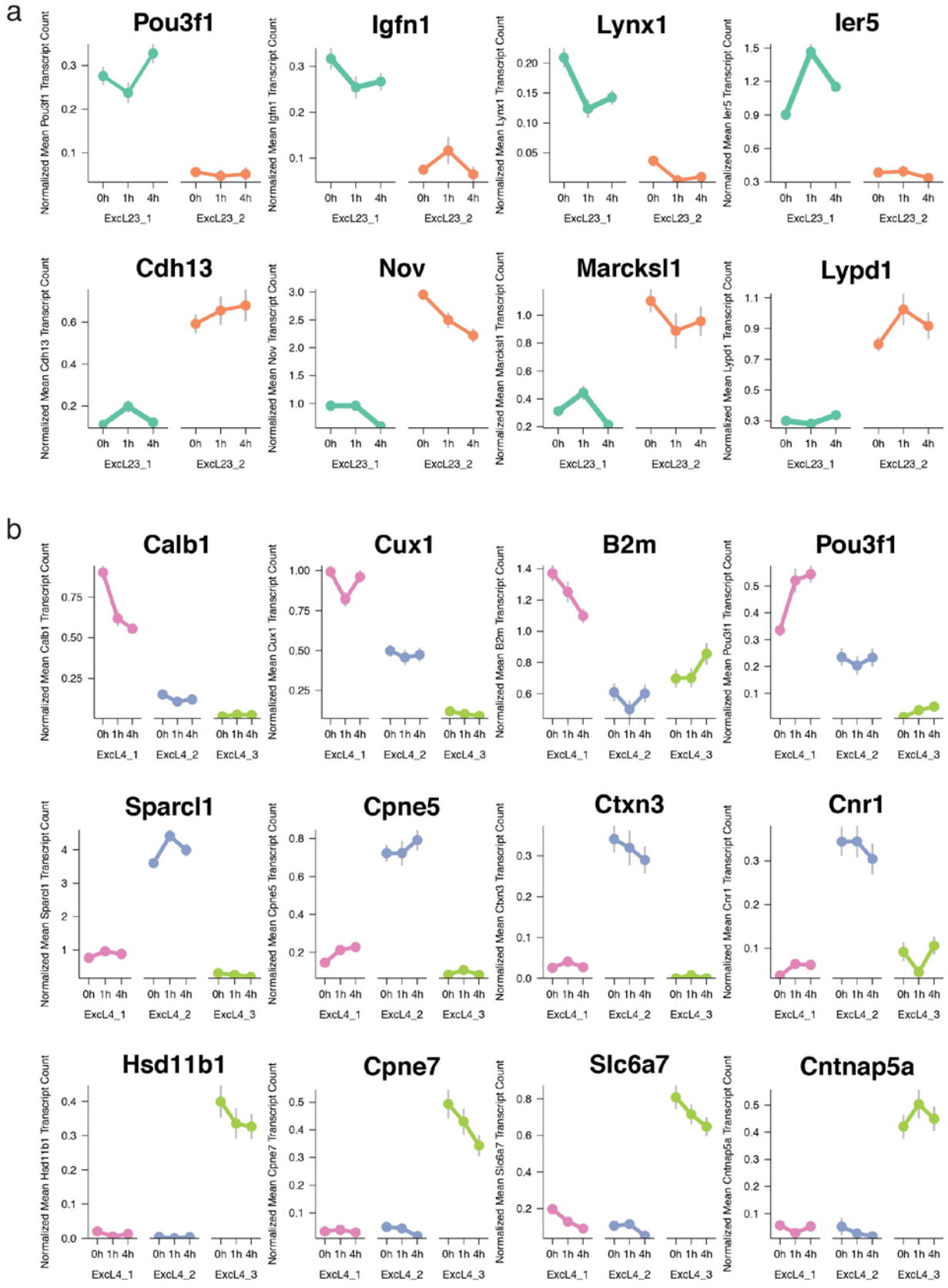
a
Pou3f1
Normalized Mean Pou3f1 Transcript Count
Igfn1
Normalized Mean Igfn1 Transcript Count
Lynx1
Normalized Mean Lynx1 Transcript Count
Ier5
Normalized Mean Ier5 Transcript Count
Cdh13
Normalized Mean Cdh13 Transcript Count
Nov
Normalized Mean Nov Transcript Count
Marcksl1
Normalized Mean Marcksl1 Transcript Count
Lypd1
Normalized Mean Lypd1 Transcript Count
0h 1h 4h
ExcL23_1
ExcL23_2
b
Calb1
Normalized Mean Calb1 Transcript Count
Cux1
Normalized Mean Cux1 Transcript Count
B2m
Normalized Mean B2m Transcript Count
Pou3f1
Normalized Mean Pou3f1 Transcript Count
Sparcl1
Normalized Mean Sparcl1 Transcript Count
Cpne5
Normalized Mean Cpne5 Transcript Count
Ctxn3
Normalized Mean Ctxn3 Transcript Count
Cnr1
Normalized Mean Cnr1 Transcript Count
Hsd11b1
Normalized Mean Hsd11b1 Transcript Count
Cpne7
Normalized Mean Cpne7 Transcript Count
Slc6a7
Normalized Mean Slc6a7 Transcript Count
Cntnap5a
Normalized Mean Cntnap5a Transcript Count
0h 1h 4h
ExcL4_1
ExcL4_2
ExcL4_3

Supplementary Figure 19

L23 and L4 excitatory subtype marker genes are not stimulus-regulated

Mean normalized expression for several non-stimulus regulated marker genes between (**a**) L23 excitatory subtypes (n_{ExcL23_1}= n_{ExcL23_2}=) and (**b**) layer 4 excitatory subtypes (n_{ExcL4_1}= n_{ExcL4_2}= n_{ExcL4_3}=). Error bars indicate s.e.m. n_{ExcL23_1}=774, 539, 907 cells; n_{ExcL23_2}=362, 166, 193 cells; n_{ExcL4_3}=136, 137, 175 cells; n_{ExcL4_1}=732, 468, 783 cells; n_{ExcL4_2}=343, 214, 210 cells for 0, 1, and 4 h timepoints respectively.

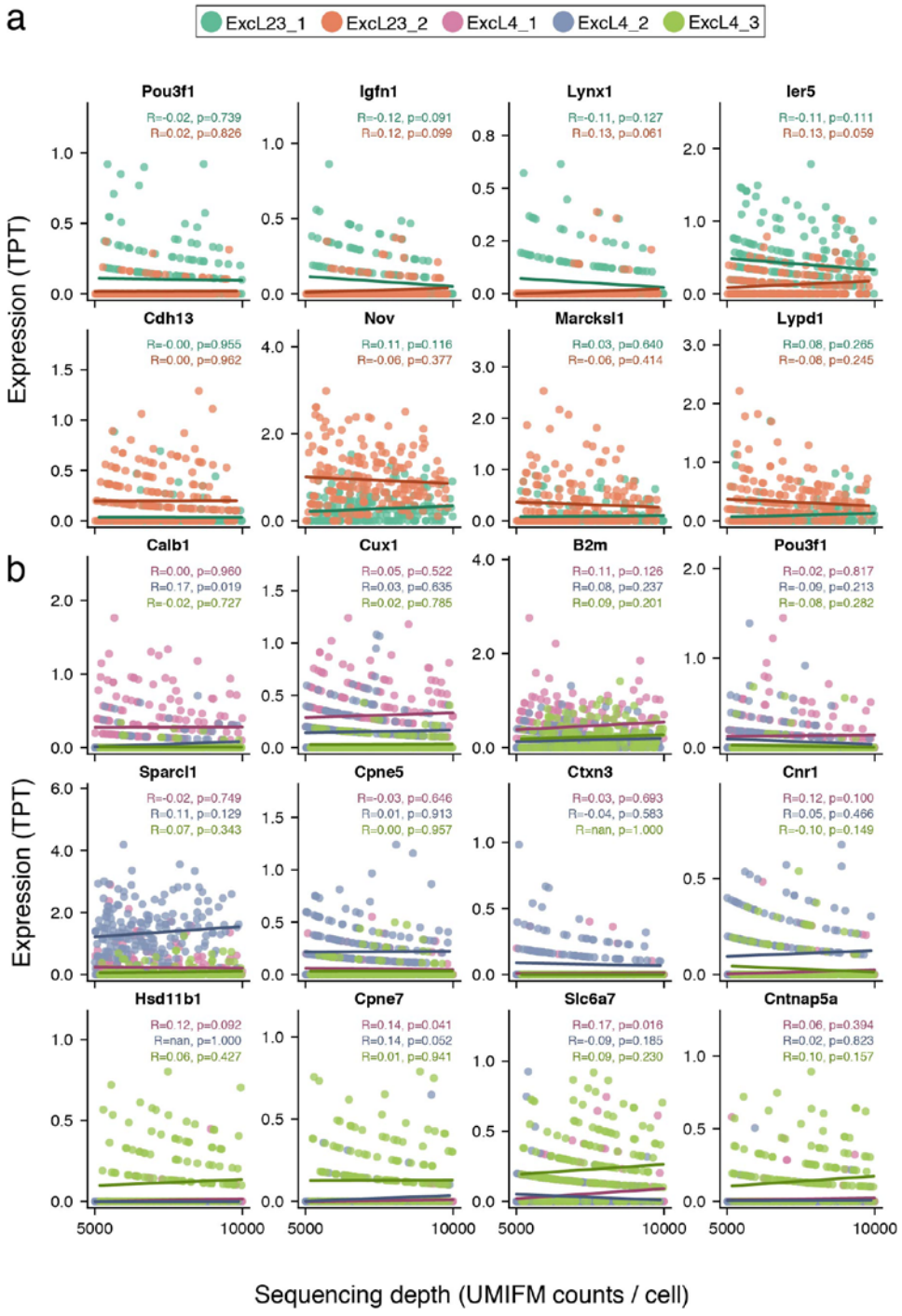
a
ExcL23_1
ExcL23_2
ExcL4_1
ExcL4_2
ExcL4_3
Pou3f1
R=-0.02, p=0.739
R=0.02, p=0.826
Igfn1
R=-0.12, p=0.091
R=0.12, p=0.099
Lynx1
R=-0.11, p=0.127
R=0.13, p=0.061
Ier5
R=-0.11, p=0.111
R=0.13, p=0.059
Cdh13
R=-0.00, p=0.955
R=0.00, p=0.962
Nov
R=0.11, p=0.116
R=-0.06, p=0.377
Marcksl1
R=0.03, p=0.640
R=-0.06, p=0.414
Lypd1
R=0.08, p=0.265
R=-0.08, p=0.245
Expression (TPT)
b
Calb1
R=0.00, p=0.960
R=0.17, p=0.019
R=-0.02, p=0.727
Cux1
R=0.05, p=0.522
R=0.03, p=0.635
R=0.02, p=0.785
B2m
R=0.11, p=0.126
R=0.08, p=0.237
R=0.09, p=0.201
Pou3f1
R=0.02, p=0.817
R=-0.09, p=0.213
R=-0.08, p=0.282
Sparcl1
R=-0.02, p=0.749
R=0.11, p=0.129
R=0.07, p=0.343
Cpne5
R=-0.03, p=0.646
R=0.01, p=0.913
R=0.00, p=0.957
Ctxn3
R=0.03, p=0.693
R=-0.04, p=0.583
R=nan, p=1.000
Cnr1
R=0.12, p=0.100
R=0.05, p=0.466
R=-0.10, p=0.149
Hsd11b1
R=0.12, p=0.092
R=nan, p=1.000
R=0.06, p=0.427
Cpne7
R=0.14, p=0.041
R=0.14, p=0.052
R=0.01, p=0.941
Slc6a7
R=0.17, p=0.016
R=-0.09, p=0.185
R=0.09, p=0.230
Cntnap5a
R=0.06, p=0.394
R=0.02, p=0.823
R=0.10, p=0.157
Expression (TPT)
5000
10000
Sequencing depth (UMIFM counts / cell)

Supplementary Figure 20

L23 and L4 subtype marker gene expression is not correlated with sequencing depth

L23 (**a**) and L4 (**b**) subtype marker gene expression (transcripts per thousand [TPT] calculated across each cell type) plotted as functions of sequencing depth (mean UMIFM counts) across 200 randomly sampled cells (with 5000≤UMIFM count/cell≤10000) within L23 and L4 respectively (markers described in **Fig. 4d**, **4e, Supplemental Fig. S19**, Online Methods). Within each plot, the lines of best fit are shown together with the calculated Pearson correlation and the associated p-value. The color of each data point or trend-line denotes the cell type represented by that object. We find that marker gene expression is not significantly correlated with sequencing depth. We also see that for each marker gene, the relative expression of the marker is appropriately greater in its marked sublayer despite restricting the sequencing depth ranges for the cells examined. This analysis confirms that the cell-type-specific expression of these marker genes is not due to differences in sequencing depth.

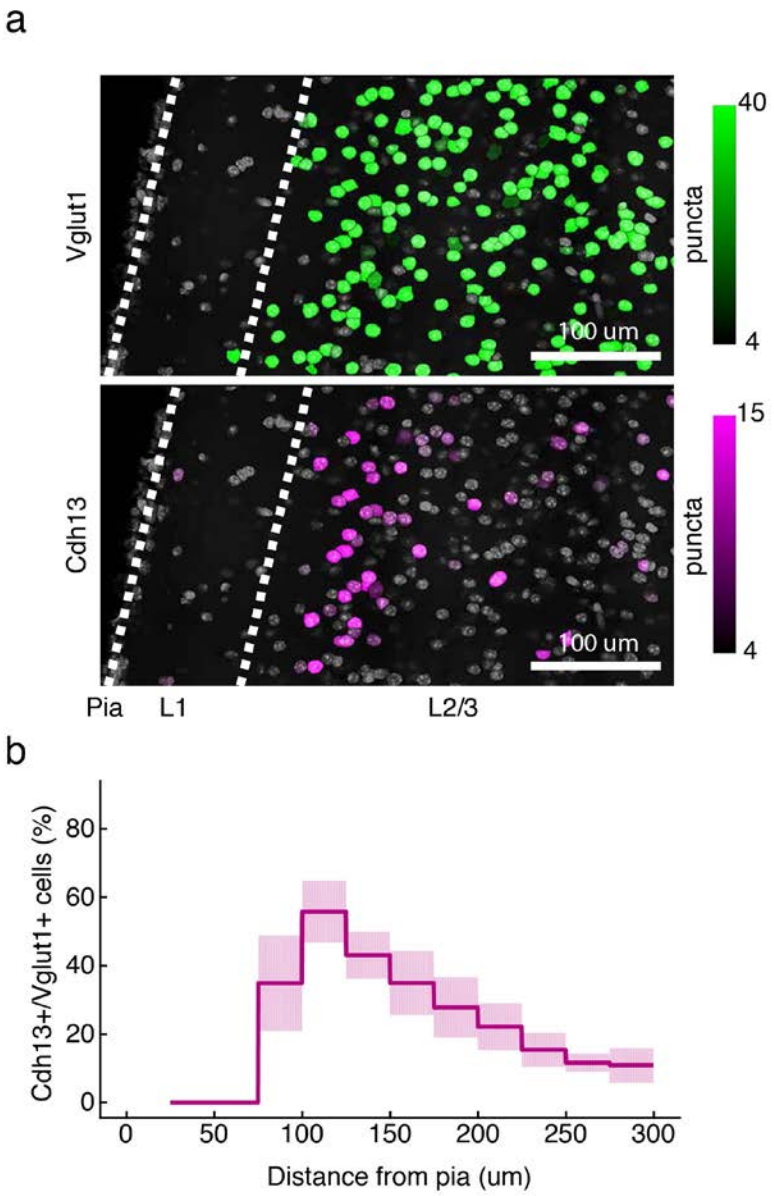

Supplementary Figure 21

***Cdh13*+ excitatory neurons are superficially enriched in layer 2/3**

(**a**) FISH images showing superficial enrichment of *Cdh13*+ cells in Layer 2/3. Nuclei are pseudo-colored by expression level of *Vglut1* (green) or *Cdh13* (magenta) FISH probes (Online methods). Scale bar=100 um.
(**b**) Quantification of FISH data showing fraction of *Cdh13*+ excitatory neurons (*Vglut1*+) as a function of distance from the pia (cells=436 *Cdh13*+/*Vglut1*+, of cells=1,624 *Vglut1*+ cells). Data from 8 cortical slices.

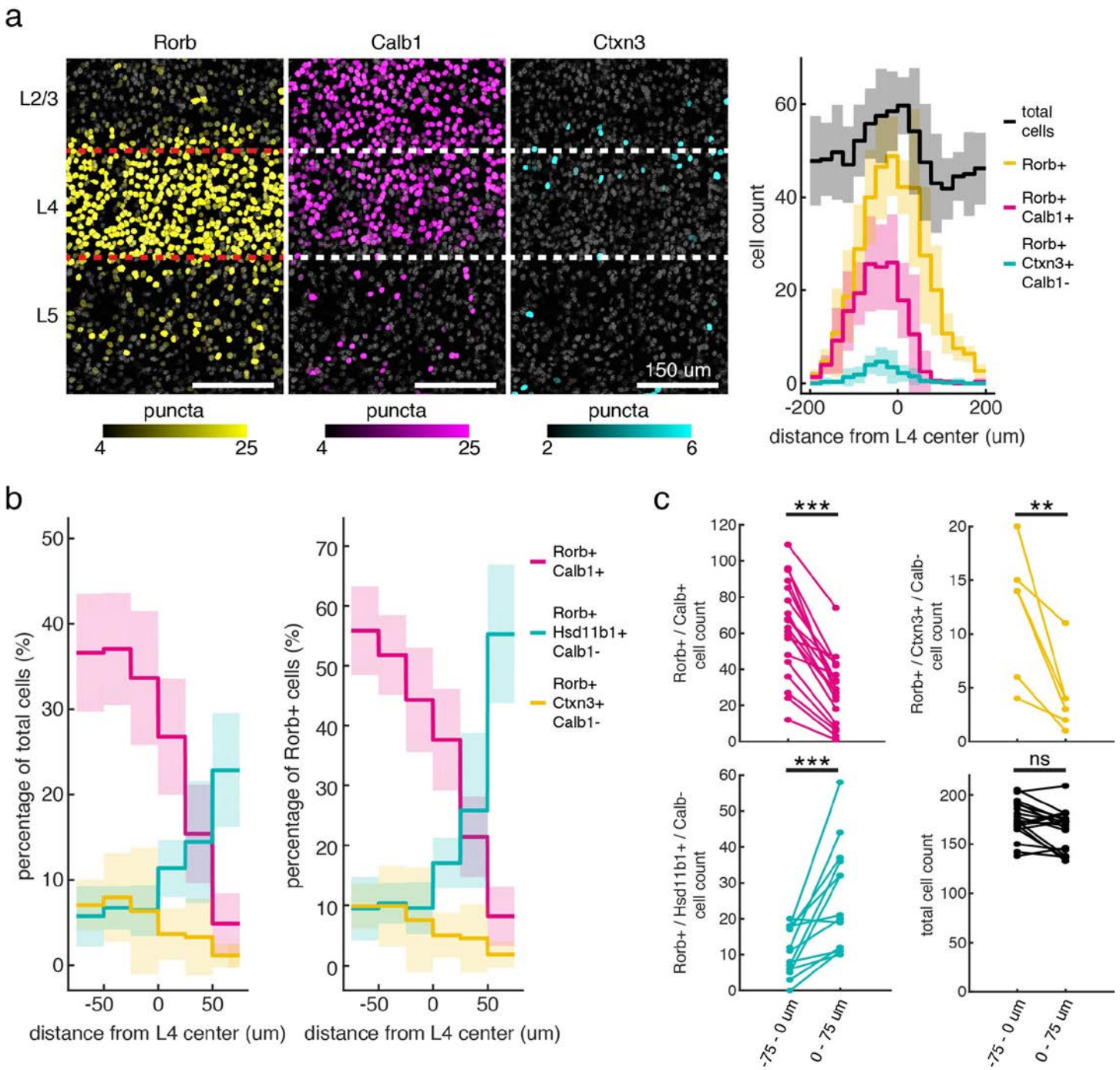

Supplementary Figure 22

FISH confirmation of L4 subtypes

(**a**) We carried out 3-color FISH for (from left) *Rorb* (yellow), *Calb1* (magenta), and *Ctxn3* (cyan). We found that *Ctxn3+/Rorb+/Calb1-* cells were intermingled with *Calb1+/Rorb+* cells superficially in layer 4. Right: summary of the anatomical distribution of the *Ctxn3* and *Calb1* transcriptionally defined cell types. Data collected from 6 slices of mouse visual cortex. Negative/positive values on x-axis correspond to distance from the center of layer 4 towards the slice surface (negative) or towards deeper cortical layers (positive). (**b**) Summary data for all layer 4 excitatory subtypes as a percentage of total cells (left), or of *Rorb+* cells (right). *Calb1+/Rorb+* and *Ctxn3+/Rorb+/Calb1-* cell types (data collected from 19 and 6 slices respectively that contained visual cortex) were enriched superficially within layer 4 by both measures, and *Hsd11b1/Rorb+/Calb1-* defined cells (data collected from 13 slices containing visual

cortex) were enriched deep within layer 4 and peaked at the border between layer 4 and 5 (see Fig. 4h). Shaded area around lines indicate 95% confidence intervals.
(**c**) Quantification of cell population enrichment to superficial (-75 to 0 um from L4 center) or deep (0 to 75 um from L4 center) layer 4. The transcriptionally defined cell types *Calb1+/Rorb+* and *Ctxn3/Rorb+/Calb1-* were significantly enriched superficially (p=0.0002, p=0.015, Mann-Whitney U-test, two-sided; data collected from 19 and 6 slices containing visual cortex, respectively), and *Hsd11b1+/Rorb+/Calb1-* cells were enriched deep within layer 4 (p=0.0034, Mann-Whitney U-test, two-sided; data collected from 13 slices containing visual cortex). On the other hand, the total number of cells in superficial and deep layer 4 was not significantly different (p=0.19, Mann-Whitney U-test, two-sided; data collected from 19 slices containing visual cortex). Scale bars=150 um. Shaded area around lines indicate 95% confidence intervals.

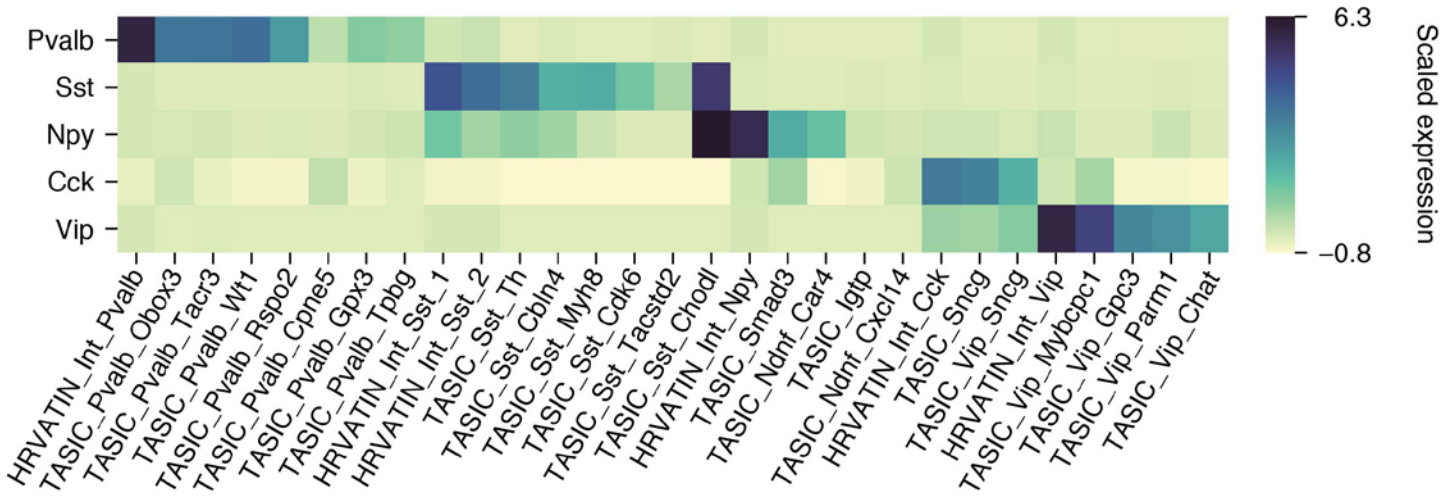

Supplementary Figure 23

Interneuron comparison between inDrops and Tasic et al. datasets
Scaled expression of interneuronal markers used to assign cell types across all interneuronal populations identified in this work and by Ref. [23]. Expression levels were scaled for each gene from each cell type independently (centered to mean with unit variance, Online Methods).

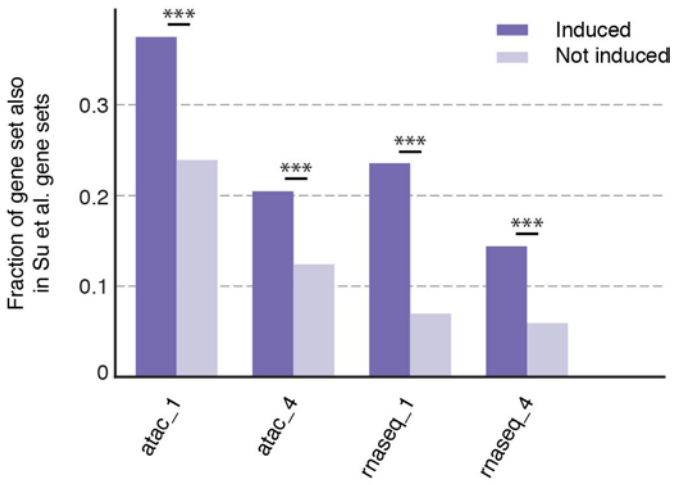

Supplementary Figure 24

V1-identified induced genes are highly enriched for genes associated with inducibly accessible loci in dentate gyrus

Induced gene sets from dentate gyrus comprising the genes with the most proximal TSS to inducibly accessible loci identified by Su *et al.* at 1 and 4 hours of stimulation (atac_1, atac_4) or the genes directly identified by Su *et al.* via bulk RNA-seq (rnaseq_1, rnaseq_4) were tested for enrichment among the induced genes identified in this study (Online Methods)[48]. The fractions of the visual cortex induced gene set identified in this study (611 genes) and its complement that were also induced in Su et al.'s paradigm are plotted. All gene sets show significant enrichment. Relative risk=1.84, 1.75, 3.67, 2.50; FDR-corrected q-value=3.2e-13, 3.4e-8, 3.4e-35, 2.7e-13 (in order shown in Figure). ***FDR-corrected q<1e-5.